

## Research Article

# Processing of Super Tough Plasticized PLA by Rotational Molding

Antonio Greco , Francesca Ferrari, and Alfonso Maffezzoli 

*Department of Engineering for Innovation, University of Salento, Via per Monteroni, 73100 Lecce, Italy*

Correspondence should be addressed to Antonio Greco; [antonio.greco@unisalento.it](mailto:antonio.greco@unisalento.it)

Received 22 October 2018; Revised 14 December 2018; Accepted 27 December 2018; Published 3 February 2019

Academic Editor: Alexandra Muñoz-Bonilla

Copyright © 2019 Antonio Greco et al. This is an open access article distributed under the Creative Commons Attribution License, which permits unrestricted use, distribution, and reproduction in any medium, provided the original work is properly cited.

This work is aimed at studying the suitability of polylactic acid (PLA) plasticized by two cardanol derivatives, i.e., cardanol and epoxidized cardanol acetate, in rotational molding, for the production of hollow items. For this purpose, plasticized PLA samples were obtained by melt mixing and then processed by a lab-scale rotational molding equipment. For comparison, poly(ethylene glycole), PEG, and plasticized PLA samples were also produced. Despite the very low cooling rates attained in rotational molding, completely amorphous samples were obtained with neat PLA and PLA plasticized by cardanol derivatives. In contrast, PEG plasticized PLA showed a very high degree of crystallinity, as highlighted by DSC and XRD analysis, which made the extraction of the rotomolded box-shaped specimens impossible. The plasticizing effectiveness of cardanol derivatives was proven by tensile testing of rotational molded prototypes, which highlighted the reduced modulus and strength and improved strain to break, compared to neat PLA. Therefore, efficient toughening of PLA can be attained by the use of the two cardanol derived plasticizers, which involves a significant reduction of the polymer glass transition, as well as a reduced increase of the crystallization kinetic. On the other hand, the reduction of the glass transition temperature due to the addition of plasticizer is responsible for significant crystallization effects even during ageing at room temperature, which involves significant embrittlement of the material.

## 1. Introduction

In recent years, the need of a valid alternative to oil-based plastics led to the development of innovative processing techniques for the production of environmentally safe poly(lactic acid), PLA. Different polymer processing technologies, such as extrusion, injection molding, calendaring, thermoforming, and fiber spinning [1, 2], have been properly adapted to the production of different PLA items. On the other hand, PLA has been shown to be a very attractive polymer for the production of hollow articles by rotational molding [3, 4]. The most relevant application, allowed by the use of PLA for rotomolding, lies in the possibility of producing a new class of eco-friendly hollow objects (e.g., pots or containers), which can be easily discarded after their usage due to the material biodegradability [5]. The low viscosity of the material promotes a very fast sintering process just above the melting temperature [6–8]. The main issue associated with the use of PLA in rotational molding is its high brittleness [9], which could prevent mold extraction. In order

to improve PLA toughness, the use of poly(ethylene glycol), PEG, plasticizer, was attempted. However, although PEG plasticized PLA processed by compression molding showed to be tougher than neat PLA [10], the same material processed by rotational molding showed a significant embrittlement compared to neat PLA, as a consequence of an increase in the rate of crystallization, finally leading to larger and more brittle crystals [11]. This is mainly related to the different cooling rates experienced by the material under different processing conditions; in particular, rotational molding is characterized by very low cooling rates [12], which promote crystallization at low undercooling leading to large crystals. On the other hand, cardanol derived plasticizers, initially proposed for the production of soft PVC [13, 14], showed to be suitable also for plasticization of PLA. Compared to PEG, cardanol derived plasticizers were shown to involve a less significant increase of the crystallization kinetics [15]. PLA plasticized by cardanol acetate processed by compression molding was characterized by higher ductility compared to PEG plasticized PLA [16]. Nevertheless, in a recent work it

was shown that raw cardanol and epoxidized cardanol acetate can act as more efficient plasticizers towards injection molded PLA compared to cardanol acetate, which was firstly used for PLA toughening [15, 17].

Therefore, this work is aimed to study the suitability of two cardanol derived plasticizers, raw cardanol and epoxidized cardanol acetate, for plasticization of PLA, aimed at the production of hollow items by rotational molding. Compared to our previous work [17], in which the very high cooling rates characteristic of injection molding allow obtaining a completely amorphous polymer, the effect of the very slow cooling rates characteristic of rotational molding is here presented.

For this purpose, different samples with 20% of plasticizer were obtained by melt mixing and processed by rotational molding. The plasticizer amount was chosen based on the results of previous work, showing that this allows obtaining the best mechanical properties, in terms of modulus reduction and ductility increase [17]. In particular, for each of the tested plasticizers, a decrease of modulus with the amount of plasticizer was found. However, a substantial difference was observed when the amount of plasticizer was varied from 10% to 20%. On the other hand, the modulus reduction was less relevant with an increase of the plasticizer amount from 20% to 30%.

Mechanical, thermal, and physical characterization of PLA plasticized by cardanol derivatives highlighted the suitability of the material for the production of void-free, highly tough hollow parts. Finally, the stability of the crystalline structure of the materials due to ageing at room temperatures was studied.

## 2. Materials and Methods

PLA, Ingeo Biopolymer 2003D, supplied by NatureWorks (Minnetonka, MN US), characterized by a density of  $1.24 \text{ g/cm}^3$ , a melt flow rate of  $6 \text{ g/600 s}$  at  $210^\circ\text{C}$ , and a D-isomer content lower than 4%, was used. Poly (ethylene glycol), PEG, with a molecular weight  $M_w = 400 \text{ g/mol}$ , was purchased from Sigma-Aldrich (St. Louis, MO, US). Technical cardanol, characterized by a purity of 95%, was purchased from Oltremare (Bologna, Italy). Epoxidized cardanol acetate (ECA) was provided by Serichim (Torviscosa, Udine, Italy) and was obtained by acetylation and further epoxidation of cardanol. The material is characterized by a yield of epoxidation of about 81% with an average molecular weight of about  $370 \text{ g/mole}$  [18, 19].

For the production of plasticized PLA, the procedure used in [17] was followed: 80 wt% PLA and 20 wt% of plasticizers were mixed in a HAAKE POLYLAB SYSTEM twin screw extruder with a 3 mm diameter rod die, using the following temperature profile from the feeder zone to the die: 190, 190, 180, 180, 165, 160, and  $140^\circ\text{C}$  and a screw speed of 15 rpm. After extrusion, materials were pelletized by a Thermo Scientific VARICUT 557-2685 pelletizer.

Rotational molded samples were obtained by a ROTO-MOULD ALPHA mod. 330\_15\_20 device, produced by Salentech. For this purpose, 300 grams of material (corresponding to a wall thickness of about 1.5 mm) was dosed in a cubic

shaped aluminum mold ( $15 \times 15 \times 15 \text{ cm}$ ) and then subjected to heating in a forced convection oven set at  $300^\circ\text{C}$ , using 1.6 rpm and 6.4 rpm for the primary and secondary axes, respectively. After 20 minutes, which allowed reaching a temperature of  $210^\circ\text{C}$  inside the mold [20], molds were extracted and cooled down for 40 minutes using a forced air convection system. For such cooling conditions, an average cooling rate in the range between  $210^\circ\text{C}$  and  $50^\circ\text{C}$  of  $4^\circ\text{C/min}$  can be estimated. The densities of rotational molded samples were measured to be in the range of  $1.22 \pm 0.04 \text{ g/cm}^3$ , without significant differences between samples. The void fraction, estimated by considering a density of fully sintered samples equal to  $1.24 \text{ g/cm}^3$ , is about  $1.5 \pm 0.03\%$  and is in the range commonly found in rotational molding of polyethylene [6, 21].

In order to test the stability of the developed products, rotational molded samples were stored in a dark place and subjected to ageing for 60 days at  $25^\circ\text{C}$ . The loss of plasticizer, measured by weighting of the samples after ageing, was found to be negligible (less than 0.1%). Instead, ageing brought significant changes in the crystalline structure, as evaluated by DSC and XRD analyses.

DSC analysis was performed on a Mettler Toledo 822 (Mettler Toledo, Greifensee, Switzerland) instrument under a nitrogen flux of  $60 \text{ mL/min}$ , applying an heating scan between  $-100^\circ\text{C}$  and  $200^\circ\text{C}$  at  $20^\circ\text{C/min}$ .

XRD analysis (Rigaku, Tokyo, Japan) was carried out with  $\text{CuK}\alpha$  radiation ( $\lambda = 1.5418 \text{ \AA}$ ) in the step scanning mode recorded in the  $2\theta$  range of  $10^\circ$ – $40^\circ$ , with a step size of  $0.02^\circ$  and step duration of 0.5s.

Tensile tests were performed on rotational molded samples on a LLoyd LR50K dynamometer according to ASTM D638 standard, using  $50 \text{ mm/min}$  crosshead speed and  $10 \times 1.5 \times 100 \text{ mm}$  samples. For each measurement, 6 specimens were used, each one extracted from one of the surfaces of the mold, in order to account for the potential change in the mechanical properties resulting from inhomogeneous heating/cooling during rotational molding. All the samples were taken at half distance between the center of the face and the border, including the sample taken from the vented surface. Due to significant embrittlement brought by the ageing process, performing tensile testing after ageing was not possible.

Due to the very high toughness of PLA samples plasticized by cardanol derivatives, it was not possible to perform impact tests (either with falling dart impact machine or with conventional Charpy/Izod equipment), since in any case no failure was observed. Therefore, the toughness of the samples, which is strictly correlated to the impact properties of the material, was estimated by tensile tests as the total area under the stress-strain curve.

## 3. Results and Discussion

DSC thermograms obtained on rotational molded samples are reported in Figure 1. Neat PLA shows three distinct transitions, starting from the low temperature, a glass transition signal at about  $56^\circ\text{C}$ , followed by cold crystallization (exothermic peak around  $105^\circ\text{C}$ ) and melting

TABLE 1: Thermal properties of rotational molded PLA.

Sample	$T_g$ (°C)	$T_c$ (°C)	$T_m$ (°C)	$H_{cc}$ (J/g)	$H_m$ (J/g)	$x_c$	$x_{cT}$
PLA	56	105	152	28	28	0	0
PLA_PEG	--	91	136	7.25	35	0.8	0.37
PLA_CARD	22	74	144	35	35	0	0
PLA_ECA	32	81	144	30	35	0.15	0.07

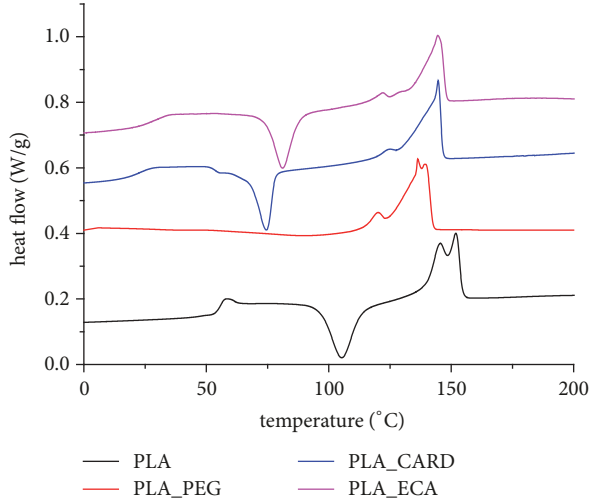


FIGURE 1: DSC on rotational molded samples.

(double endothermic peak around 150°C). The latent heat associated with cold crystallization, reported in Table 1, is equal to the latent heat of melting, indicating that at room temperature the sample is completely amorphous. Therefore, even in presence of the very low cooling rates characteristic of rotational molding, PLA is not able to crystallize, which is due to a very low rate of crystallization of the specific grade used in this work [3, 11, 15]. In contrast, the sample PLA\_PEG is characterized by a very high degree of crystallinity, as evidenced by the absence of any detectable glass transition signal, and the very weak cold crystallization peak. Therefore, it is possible to estimate an initial degree of crystallinity  $x_c=0.8$  as

$$x_c = \frac{H_{mc}}{H_m} = \frac{H_m - H_{cc}}{H_m} \quad (1)$$

where  $H_{mc}$  is the melt crystallization enthalpy, corresponding to the unknown enthalpy released by the material during processing;  $H_{cc}$  and  $H_m$  are the cold crystallization and melting enthalpies measured during the DSC scan and reported in Table 1. The relation of (1) holds in the assumption that  $H_m = H_{mc} + H_{cc}$ ; the melting enthalpy is the sum of the melt crystallization and cold crystallization enthalpy. The melting peak is shifted at lower temperatures (136°C), as a consequence of the plasticizing effect of PEG, according to the Flory-Huggins theory [22].

Alternatively, the degree of crystallinity of PLA was obtained by dividing the melting enthalpy of PLA by the theoretical melting enthalpy of a completely crystalline PLA,

which is 93.0 J/g [23], corrected by the weight fraction of PLA in each sample,  $w_{PLA}$ :

$$x_{cT} = \frac{H_{mc}}{w_{PLA} * 93 [J/g]} = \frac{H_m - H_{cc}}{w_{PLA} * 93 [J/g]} \quad (2)$$

where  $w_{PLA}$  is 1 for neat PLA and 0.8 for plasticized PLA. Results obtained by the use of (2) are also reported in Table 1.

The behavior of PLA\_CARD is substantially similar to that of neat PLA: the heat of cold crystallization is equal to that of melting, which indicates that rotational molded samples are completely amorphous. On the other hand, compared to neat PLA, the significant transitions of PLA\_CARD are shifted at lower temperatures, as reported in Table 1: the glass transition temperature is 22°C, which indicates the plasticizing effectiveness of CARD, the cold crystallization peak is also shifted from 105°C to 74°C, which indicates the enhanced mobility brought by the addition of the plasticizer, promoting a faster crystallization compared to neat PLA, and the melting temperature is shifted from 152°C to 144°C, which is a direct consequence of plasticization, according to the Flory-Huggins theory. The DSC thermogram of PLA\_ECA shows an intermediate behavior: above glass transition, which is centered at 32°C, the material shows cold crystallization, which is, however, characterized by a lower area compared to melting. In particular, the initial degree of crystallinity of PLA\_ECA, was estimated to be  $x_c=0.15$  by (1). Compared to (1), the results obtained by the use of (2) yield lower value of the degree of crystallinity, however, still confirming the most relevant result, i.e., the increased degree of crystallinity brought by the addition of the plasticizers.

A further conclusion from the data of Table 1 is that all the plasticizers increase the maximum attainable degree of crystallinity, as evidenced by the much higher value of the melting enthalpy compared to neat PLA

The glass transition temperature reduction, which is the expected effect of the addition of the plasticizer and is responsible for PLA toughening, poses some doubts about the stability of the thermal and mechanical properties of the developed materials. This is of major concern also in view of the fact that the glass transition region is very close to room temperature, which can lead to some morphological changes even under room conditions. The DSC thermograms of rotational molded samples after ageing for 60 days at 25°C are reported in Figure 2 and the corresponding values measured for the transition temperatures and enthalpies are reported in Table 2. After ageing, sample PLA\_PEG and PLA\_CARD do not show any glass transition signal and cold crystallization peak, indicating the occurrence of significant recrystallization during ageing, leading to the formation of

TABLE 2: Thermal properties of rotational molded aged PLA.

Sample	$T_g$ (°C)	$T_c$ (°C)	$T_m$ (°C)	$H_{cc}$ (J/g)	$H_m$ (J/g)	$x_c$
PLA_PEG	-	-	136	0	35	1
PLA_CARD	-	-	142	0	35	1
PLA_ECA	31	83	146	28	35	0.19

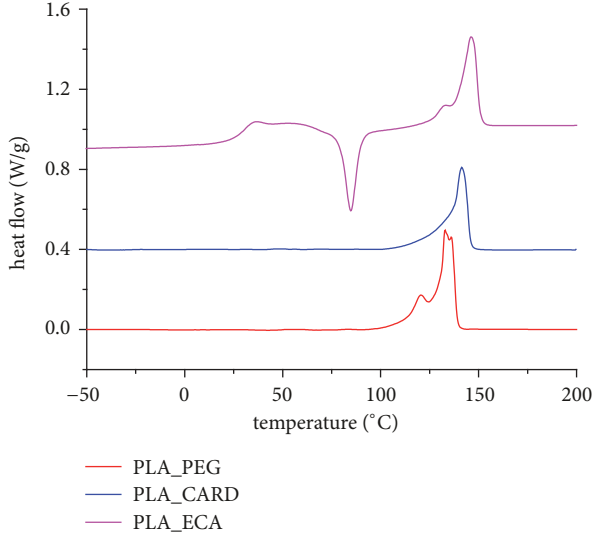


FIGURE 2: DSC on rotational molded aged samples.

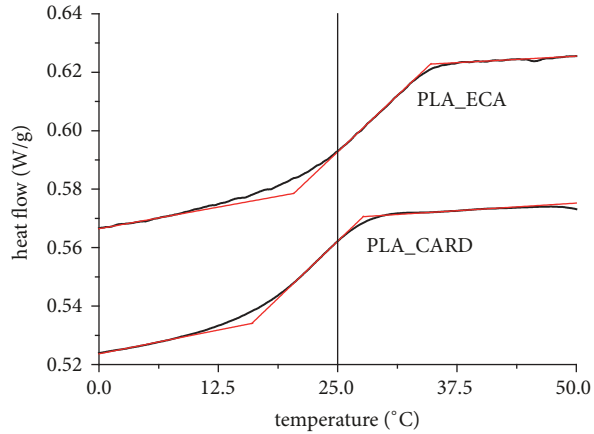


FIGURE 3: Glass transition signal and tensile testing temperature.

a completely crystalline structure. Sample PLA\_ECA shows almost unchanged values of glass transition and melting temperatures compared to the as-produced sample. Only a slight decrease of the cold crystallization enthalpy is indicative of an increase of the degree of crystallinity due to ageing.

The different behavior for sample PLA\_CARD and PLA\_ECA during ageing can be understood by referring to the results of Figure 3, which represent the DSC curves of the two materials before ageing in the glass transition region. At each temperature, the fraction of material which is in the

amorphous rubbery state,  $x_{rubbery}$ , can be estimated from the specific heat,  $c_p$ , according to

$$c_p(T) = c_{p,rubbery}x_{rubbery} + c_{p,glassy}(1 - x_{rubbery}) \quad (3)$$

where  $c_{p,rubbery}$  and  $c_{p,glassy}$  are the specific heats corresponding to a completely rubbery and completely glassy samples, respectively. From linearization of the DSC signal, being

$$c_p(T) = A_{flex} + B_{flex}T$$

$$c_{p,glassy}(T) = A_{flex} + B_{flex}T_{onset} \quad (4)$$

$$c_{p,rubbery}(T) = A_{flex} + B_{flex}T_{endset}$$

where  $A_{flex}$  and  $B_{flex}$  are the linearization coefficients in the inflection point, it can be estimated that the amount of material  $x_{rubbery}$  which is above its glass transition is given as:

$$x_{rubbery}(T) = \frac{T - T_{onset}}{T_{endset} - T_{onset}} \quad (5)$$

For CARD, the endset and onset of the glass transition have been calculated as  $T_{onset}=16^\circ\text{C}$  and  $T_{endset}=27.7^\circ\text{C}$ , whereas, for ECA,  $T_{onset}=20.4^\circ\text{C}$  and  $T_{endset}=34.8^\circ\text{C}$ . At room temperature ( $25^\circ\text{C}$ ), according to (5), about 77% of PLA\_CARD is above the its glass transition, whereas only about 32% of PLA\_ECA is above its glass transition; therefore, at  $25^\circ\text{C}$ , the mobility of PLA molecules in PLA\_CARD is much higher, which involves faster recrystallization.

The crystalline structure of the molded PLA samples was confirmed by XRD analysis results, reported in Figure 4. For each sample, two different curves are reported, one obtained by XRD analysis on the external surface of the molded part, corresponding to the mold side, and the other on the internal surface of molded part, corresponding to the air side. The two surfaces experience different cooling conditions during processing: a faster cooling, due to direct contact with the mold, for the outer surface, and a slower cooling, due to the very slow heat transfer, for the inner surface [12]. The results reported in Figure 4(a) for neat PLA confirm the amorphous nature of the material on both surfaces, as highlighted by the wide halo band, and the absence of any relevant diffraction peak. PLA\_PEG, as reported in Figure 4(b), shows a very sharp peak at  $2\theta=16.6^\circ$  and a second peak at  $2\theta=18.8^\circ$ , which are assigned to the crystal planes (200)/(110) and (203) of the  $\alpha$  form, respectively [24, 25]. Referring to the peak at  $16.6^\circ$ , the intensity measured on the inner surface of the mold is much higher than that observed on the outer surface of the mold, indicating a higher degree of crystallinity due to the slower cooling rates during processing. PLA\_CARD shows a behavior similar to that of neat PLA, i.e., a completely

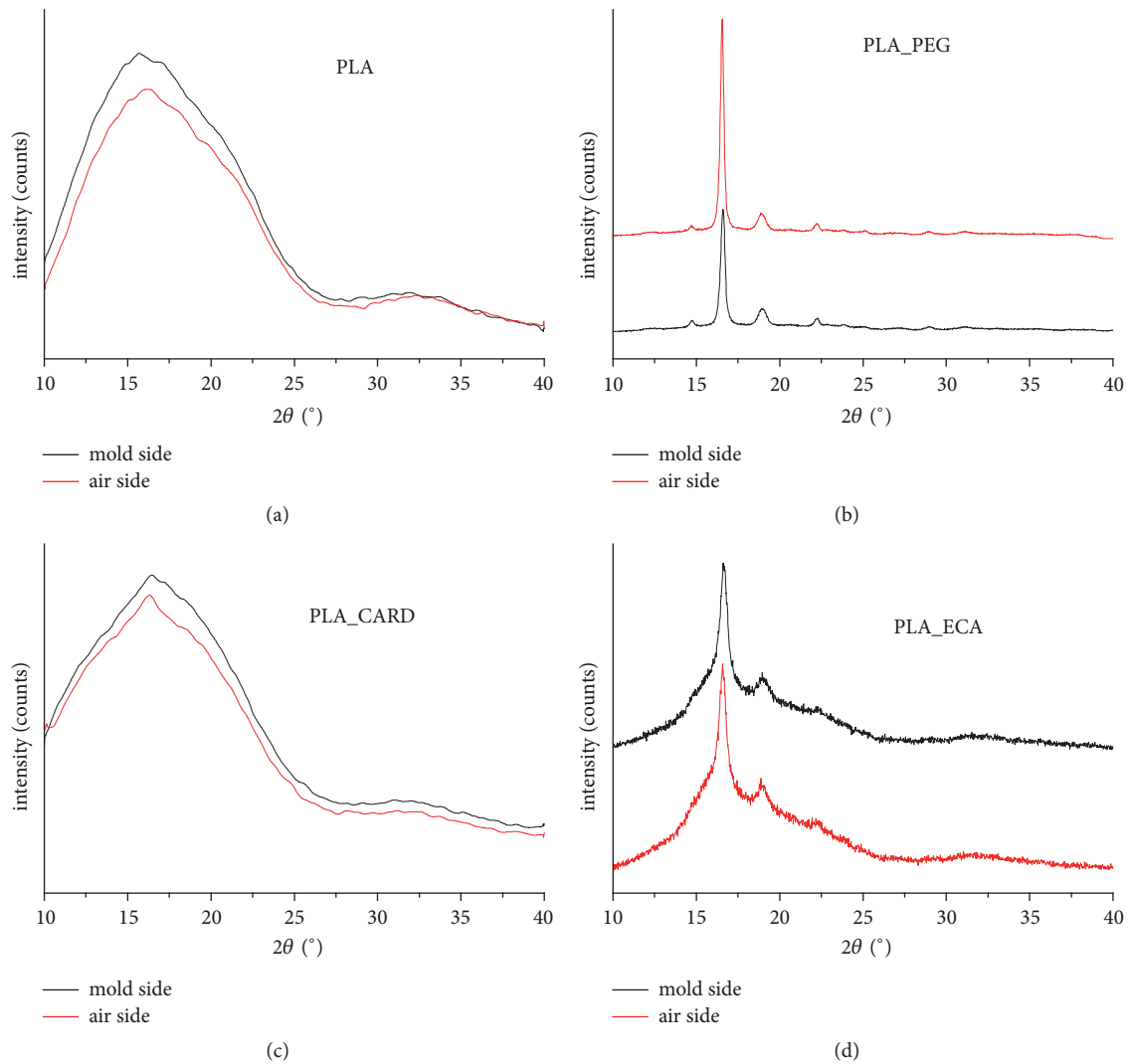


FIGURE 4: XRD diffraction patterns obtained on rotational molded PLA samples: (a) neat PLA, (b) PEG plasticized PLA, (c) cardanol plasticized PLA, and (d) epoxidized cardanol acetate plasticized PLA.

amorphous structure, whereas PLA\_ECA shows the presence of crystalline peak at  $2\theta=16.6^\circ$  and  $2\theta=18.8^\circ$ , overlapping with the halo band, which is indicative of the formation of a semicrystalline structure.

The XRD diffraction patterns of molded samples were used for estimating the degree of crystallinity, as the ratio between the area of the peaks at  $16.6^\circ$  and  $18.8^\circ$ , and the total area of the XRD pattern, including the amorphous halo band. The results are reported in Figure 5 and compared to the results from DSC analysis. As can be observed, the results from XRD and DSC analysis are in substantial good agreement, being PLA\_PEG characterized by a very high degree of crystallinity. As expected, the outer surface of molded sample is characterized by a lower degree of crystallinity compared to the inner surface. After ageing, PLA\_PEG reaches a unitary degree of crystallinity. PLA\_CARD, obtained by rotational molding, is fully amorphous, either from DSC or from XRD analysis; instead, the degree of crystallinity significantly increases due to ageing. The results of Figure 5 for PLA\_ECA

highlight the different structure of outer surface and inner surface of molded products, as well as the limited increase of crystallinity brought by ageing.

Typical stress-strain curves of molded plasticized PLA samples are reported in Figure 6, and the corresponding mechanical properties are reported in Figures 7(a)–7(d). Samples PLA\_PEG were not tested, due to their high brittleness, resulting from the very high degree of crystallinity, which did not allow for extraction from the mold after processing. Analogously, no characterization was performed after ageing: even in this case, the very high brittleness of the materials did not allow for mechanical characterization.

In particular, referring to Figure 7, neat PLA is characterized by mechanical properties comparable to those reported in the producer technical data sheet and in a previous work [11], which confirm that void-free samples were molded. On the other hand, addition of both plasticizers leads to a strong reduction of the modulus, as clearly observed in the inset at low deformations in Figures 6 and 7(a). A detailed

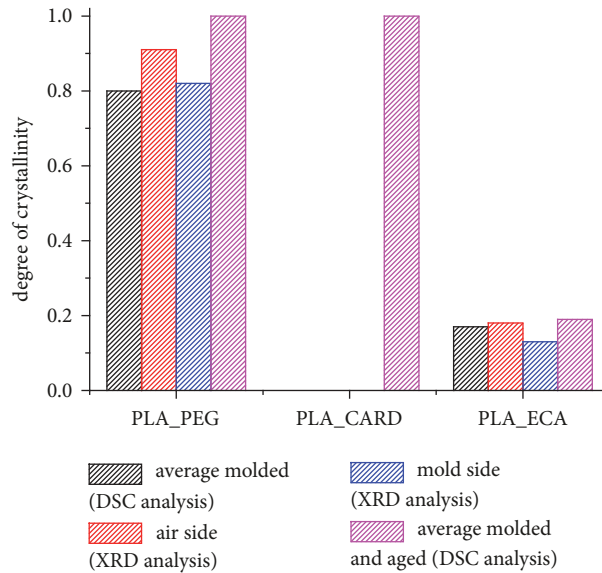


FIGURE 5: Degree of crystallinity for molded and aged samples estimated from DSC and XRD analysis.

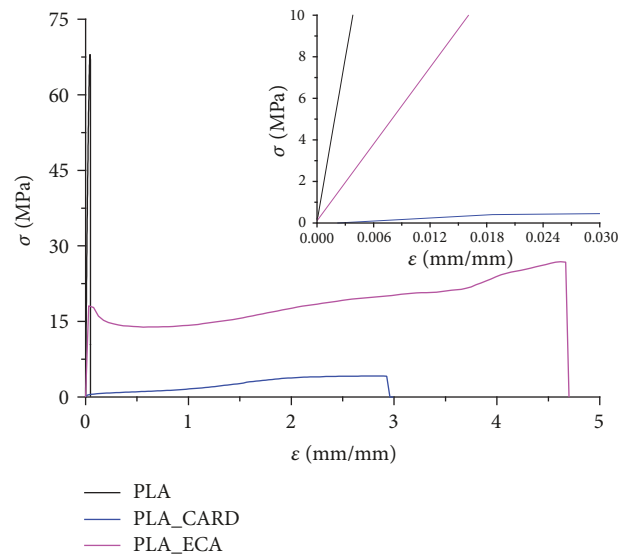


FIGURE 6: Stress-strain curves of rotational molded plasticized PLA.

discussion about the dependence of mechanical properties on the changes in the glass transition temperature and crystallization kinetics is reported in [17]. Tensile strength also decreases while strain at break increases, as observed in Figures 7(b) and 7(c). In particular, the very low modulus (83 MPa) and strength (4 MPa) of PLA\_CARD indicate a rubbery behavior, with mechanical properties comparable to those of cardanol plasticized PVC [18, 19, 26]. Compared to PLA\_CARD, the higher modulus and strength of PLA\_ECA, which are measured to be 410 MPa and 23 MPa, respectively, are attributed to the semicrystalline structure of the latter, compared to the amorphous structure of the former. In addition, referring to Figure 3, in correspondence of the temperature of tensile testing, 25°C, most of PLA\_CARD is above its glass transition, whereas most of PLA\_ECA is

below its glass transition, which also contributed to the higher brittleness of PLA\_ECA compared to PLA\_CARD. Finally, in Figure 7(d) the toughness, obtained as the total area under the stress-strain curve, is reported. Addition of cardanol and epoxidized cardanol acetate to neat PLA allows increasing the toughness from 1.7  $\text{mJ}/\text{mm}^3$  to 7.8  $\text{mJ}/\text{mm}^3$  and to 91  $\text{mJ}/\text{mm}^3$ , respectively.

#### 4. Conclusions

In this work, suitability of cardanol and epoxidized cardanol acetate for the plasticization of PLA during rotational molding process has been assessed. An amount of 20% by weight of cardanol added to PLA leads to a decrease the glass transition temperature of PLA, without any increase of the degree of

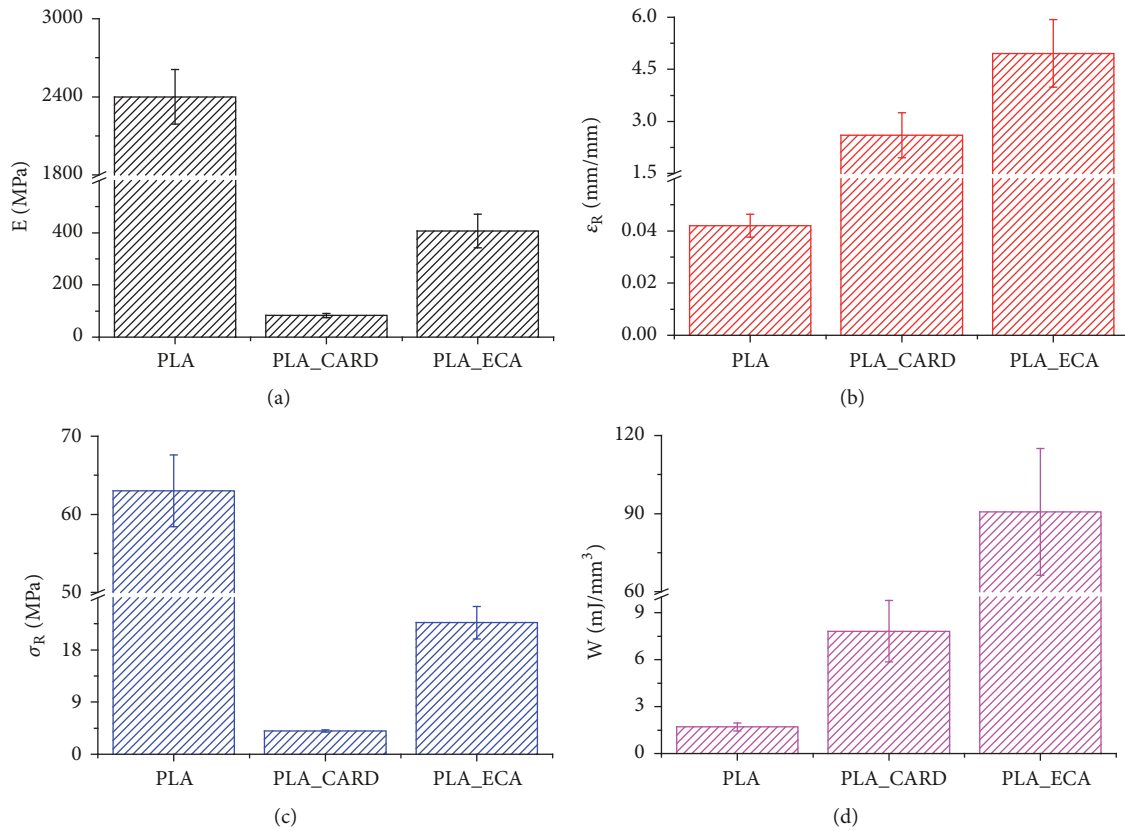


FIGURE 7: Mechanical properties of rotational molded plasticized PLA: (a) tensile modulus, (b) strain at break, (c) tensile strength, and (d) toughness.

crystallinity, which leads to the formation of a completely amorphous structure. On the other hand, the addition of PEG is responsible for the development of a high degree of crystallinity at the cooling rates typically found in rotational molding, involving a dramatic embrittlement of the material. Addition of epoxidized cardanol acetate leads to the development of a semicrystalline structure, characterized by a degree of a much lower crystallinity, compared to the one attained by the use of PEG. The resulting PLA items are characterized by much lower modulus and strength compared to neat PLA, as well as an increased strain at break and toughness. In particular, the higher plasticizing effectiveness of cardanol is highlighted by the lower modulus and strength compared to epoxidized cardanol acetate. Nevertheless, the very tough plasticized PLA obtained is characterized by significant recrystallization effects occurring for sufficiently long times even at low temperatures; such recrystallization is responsible for a significant embrittlement, which poses some issues related to potential applications of the developed material.

### Data Availability

There is no underlying data to this paper

### Conflicts of Interest

The authors declare that they have no conflicts of interest.

### References

- [1] L.-T. Lim, R. Auras, and M. Rubino, "Processing technologies for poly(lactic acid)," *Progress in Polymer Science*, vol. 33, no. 8, pp. 820–852, 2008.
- [2] S. K. Pankaj, C. Bueno-Ferrer, N. N. Misra et al., "Characterization of polylactic acid films for food packaging as affected by dielectric barrier discharge atmospheric plasma," *Innovative Food Science and Emerging Technologies*, vol. 21, pp. 107–113, 2014.
- [3] A. Greco and A. Maffezzoli, "Rotational Molding of Poly(lactic acid): Effect of Polymer Grade and Granulometry," *Advances in Polymer Technology*, vol. 36, no. 4, pp. 477–482, 2017.
- [4] E. Cisneros-López, A. Pérez-Fonseca, Y. González-García et al., "Polylactic acid–agave fiber biocomposites produced by rotational molding: A comparative study with compression molding," *Advances in Polymer Technology*, vol. 37, no. 7, pp. 2528–2540, 2017.
- [5] A. Greco, A. Maffezzoli, and S. Forleo, "Sintering of PLLA powders for rotational molding," *Thermochimica Acta*, vol. 582, pp. 59–67, 2014.
- [6] A. Greco and A. Maffezzoli, "Powder-Shape Analysis and Sintering Behavior of High-Density Polyethylene Powders for Rotational Molding," *Journal of Applied Polymer Science*, vol. 92, no. 1, pp. 449–460, 2004.
- [7] A. Greco and A. Maffezzoli, "Polymer melting and polymer powder sintering by thermal analysis," *Journal of Thermal Analysis and Calorimetry*, vol. 72, no. 3, pp. 1167–1174, 2003.

- [8] M. Kontopoulou and J. Vlachopoulos, "Melting and densification of thermoplastic powders," *Polymer Engineering & Science*, vol. 41, no. 2, pp. 155–169, 2001.
- [9] M. Murariu, A. Da Silva Ferreira, M. Alexandre, and P. Dubois, "Polylactide (PLA) designed with desired end-use properties: 1. PLA compositions with low molecular weight ester-like plasticizers and related performances," *Polymers for Advanced Technologies*, vol. 19, no. 6, pp. 636–646, 2008.
- [10] Y.-P. Song, D.-Y. Wang, X.-L. Wang, L. Lin, and Y.-Z. Wang, "A method for simultaneously improving the flame retardancy and toughness of PLA," *Polymers for Advanced Technologies*, vol. 22, no. 12, pp. 2295–2301, 2011.
- [11] A. Greco and A. Maffezzoli, "Analysis of the suitability of polylactic acid in rotational molding," *Polymers for Advanced Technologies*, vol. 34, no. 3, p. 21505, 2015.
- [12] A. Greco, A. Maffezzoli, and J. Vlachopoulos, "Simulation of Heat Transfer during Rotational Molding," *Advances in Polymer Technology*, vol. 22, no. 4, pp. 271–279, 2003.
- [13] A. Greco, F. Ferrari, R. Del Sole, and A. Maffezzoli, "Use of cardanol derivatives as plasticizers for PVC," *Journal of Vinyl and Additive Technology*, vol. 24, pp. E62–E70, 2018.
- [14] A. Greco, F. Ferrari, R. Velardi, M. Frigione, and A. Maffezzoli, "Solubility and durability of cardanol derived plasticizers for soft PVC," *International Polymer Processing*, vol. 31, no. 5, pp. 577–586, 2016.
- [15] A. Greco, F. Ferrari, and A. Maffezzoli, "Thermal analysis of poly(lactic acid) plasticized by cardanol derivatives," *Journal of Thermal Analysis and Calorimetry*, vol. 134, no. 1, pp. 559–565, 2018.
- [16] A. Greco and A. Maffezzoli, "Cardanol derivatives as innovative bio-plasticizers for poly-(lactic acid)," *Polymer Degradation and Stability*, vol. 132, pp. 213–219, 2016.
- [17] A. Greco, F. Ferrari, and A. Maffezzoli, "Mechanical properties of poly(lactid acid) plasticized by cardanol derivatives," *Polymer Degradation and Stability*, vol. 159, pp. 199–204, 2019.
- [18] A. Greco, D. Brunetti, G. Renna, G. Mele, and A. Maffezzoli, "Plasticizer for poly(vinyl chloride) from cardanol as a renewable resource material," *Polymer Degradation and Stability*, vol. 95, no. 11, pp. 2169–2174, 2010.
- [19] A. Greco, F. Ferrari, A. Maffezzoli et al., "Solubility and durability of cardanol derived plasticizers for soft PVC," *Environmental Engineering and Management Journal*, vol. 15, no. 9, pp. 1989–1995, 2016.
- [20] A. Greco, A. Maffezzoli, and S. Forleo, "Rotational molding of bio-polymers," in *Proceedings of the 29th International Conference of the Polymer Processing Society, PPS 2013*, vol. 1593, pp. 333–337, Germany, July 2014.
- [21] E. S. Barboza Neto, L. A. F. Coelho, M. M. C. Forte, S. C. Amico, and C. A. Ferreira, "Processing of a lldpe/hdpe pressure vessel liner by rotomolding," *Materials Research*, vol. 17, no. 1, pp. 236–241, 2014.
- [22] M. Muthukumar, "Nucleation in Polymer Crystallization," in *Advances in Chemical Physics*, S. A. Rice, Ed., p. 128, John Wiley & Sons, Hoboken, NJ, USA, 2004.
- [23] D. Battagazzore, S. Bocchini, and A. Frache, "Crystallization kinetics of poly(lactic acid)-talc composites," *Express Polymer Letters*, vol. 5, no. 10, pp. 849–858, 2011.
- [24] X. Zhang, K. Schneider, G. Liu et al., "Structure variation of tensile-deformed amorphous poly(l-lactic acid): Effects of deformation rate and strain," *Polymer Journal*, vol. 52, no. 18, pp. 4141–4149, 2011.
- [25] A. Greco and A. Maffezzoli, "Rotational molding of biodegradable composites obtained with PLA reinforced by the wooden backbone of opuntia ficus indica cladodes," *Journal of Applied Polymer Science*, vol. 132, no. 48, Article ID 42447, 2015.
- [26] A. Greco, F. Ferrari, and A. Maffezzoli, "UV and thermal stability of soft PVC plasticized with cardanol derivatives," *Journal of Cleaner Production*, vol. 164, pp. 757–764, 2017.



